Accepted Manuscript

The NMR 'split peak effect' in cell suspensions: historical perspective, explanation and applications

Philip W. Kuchel, Kiaran Kirk, Dmitry Shishmarev

PII: S0079-6565(17)30053-5
DOI: https://doi.org/10.1016/j.pnmrs.2017.11.002
Reference: JPNMRS 1448

To appear in: *Progress in Nuclear Magnetic Resonance Spectroscopy*

Received Date: 4 October 2017
Accepted Date: 2 November 2017

Please cite this article as: P.W. Kuchel, K. Kirk, D. Shishmarev, The NMR 'split peak effect' in cell suspensions: historical perspective, explanation and applications, *Progress in Nuclear Magnetic Resonance Spectroscopy* (2017), doi: https://doi.org/10.1016/j.pnmrs.2017.11.002

The NMR 'split peak effect' in cell suspensions: historical perspective, explanation and applications

Philip W. Kuchel[a]*, Kiaran Kirk[b], and Dmitry Shishmarev[a,c]

[a]*The University of Sydney, School of Life and Environmental Sciences, Faculty of Science, Sydney, NSW 2006, Australia*

[b]*Australian National University, Research School of Biology, College of Science, Canberra, ACT 2601, Australia*

[c]*Australian National University, John Curtin School of Medical Research, College of Health and Medicine, Canberra, ACT 2601, Australia*

Running title: NMR 'split peaks' in cells

Correspondence: Professor Philip W. Kuchel
School of Life and Environmental Sciences
Building G08
The University of Sydney
New South Wales 2006
Australia
Email: philip.kuchel@sydney.edu.au

Key words: ^{1}H, ^{13}C, ^{19}F, ^{31}P, ^{133}Cs NMR; red blood cells; erythrocytes; hydrogen bond; magnetic susceptibility; solvent effect

ABSTRACT

The physicochemical environment inside cells is distinctly different from that immediately outside. The selective exchange of water, ions, and molecules across the cell membrane, mediated by integral, membrane-embedded proteins is a hallmark of living systems. There are various methodologies available to measure the selectivity and rates (kinetics) of such exchange processes, including several that take advantage of the non-invasive nature of NMR spectroscopy. A number of solutes, including particular inorganic ions, show distinctive NMR behaviour, in which separate resonances arise from the intra- and extracellular solute populations, without the addition of shift reagents, differences in pH, or selective binding

partners. This 'split peak effect/phenomenon', discovered in 1984, has become a valuable tool, used in many NMR studies of cellular behaviour and function. The explanation for the phenomenon, based on the differential hydrogen bonding of the reporter solutes to water, and the various ways in which this phenomenon has been used to investigate aspects of cellular biochemistry and physiology, are the topics of this review.

Contents

1. Introduction

1.1. Serendipity

The discovery of the transmembrane NMR 'split peak effect/phenomenon' [1, 2], which has its origins in different extents of hydrogen bonding of water to a reporter solute inside and outside cells, was a case of classical serendipity. In 1984, an undergraduate research-project student, KK, working with PWK, began investigating the possibility of measuring the membrane potential of cells, using the favourable non-invasive characteristics of ^{31}P NMR spectroscopy. ^{31}P NMR had been used over the previous decade to study cell and tissue metabolism: initial applications had been with intact rabbit red blood cells (RBCs) to provide an estimate of intracellular pH and measure the concentration of the metabolite 2,3-bisphosphoglycerate (2,3BPG) [3], followed a year later by ^{31}P NMR observations of pH and metabolite levels inside intact rat muscle [4].

1.2. Background and motivation

The enticement to develop an NMR method for estimating membrane potential came from reports of electrochromic dyes being used with optical spectrophotometry for that purpose. Such dyes physically exchange between the hydrophobic environment of phospholipid bilayers enclosing the cytoplasm and the aqueous medium, and their optical absorption and emission spectra are functions of the cell's membrane potential [5, 6]. We speculated that it might be possible to develop an NMR counterpart of this experiment, relying on the fact that an atomic nucleus has a resonance frequency, ω, that is directly proportional to the average strength of the local magnetic field at the nucleus, B_{loc}, as encapsulated in the Larmor equation:

$$\omega = -\gamma B_{loc} \quad (1)$$

where γ is the magnetogyric ratio of the nucleus [7, 8]. For a nucleus placed within the magnetic field (B_0) of an NMR spectrometer, the electron cloud that surrounds the nucleus partially shields it from B_0. This has the effect of lowering the resonance frequency of the nucleus. Because the changes in frequency are relatively small, and in order to normalize the

measurement and to make the changes independent of the particular magnetic field strength, the 'chemical shift' in units of ppm (parts per million) is defined as:

$$\delta = \frac{\omega_{\text{sample}} - \omega_{\text{reference}}}{\omega_{\text{reference}}} \times 10^6 \qquad (2)$$

where ω_{sample} is the resonance frequency of the nucleus of interest, and $\omega_{\text{reference}}$ is the resonance frequency of a particular nucleus in a chemical species that is chosen to be the chemical shift reference. A perturbation of the electron cloud by a change in the physicochemical environment associated with an alteration in the cell's membrane potential might be expected to alter the chemical shift of the nucleus.

Our initial intention was to use selected electrochromic dyes, hoping that NMR spectra arising from these compounds would display changes in chemical shift when the membrane potential was changed. Optical frequencies change when the membrane potential changes, so why not NMR frequencies? But, are the dyes detectable by NMR spectroscopy under cellular conditions? Unfortunately, "No!". The dye concentrations typically used are in the μM range, and NMR spectroscopy is not sufficiently sensitive to detect solutes at such low concentrations, generally requiring mM levels. Nevertheless, the notion of the physicochemical environment in and around cells affecting the NMR resonance frequency of probe nuclei remained an intriguing one.

2. Dimethyl methylphosphonate – the beginning with ^{31}P NMR

As a first step towards devising a quantitative procedure for detecting changes in chemical shifts of selected probe solutes in RBCs, we sought a new chemical shift and intensity reference-compound that would dissolve in an aqueous medium while not perturbing cellular metabolism. Up to this time, there had been no universally applicable internal references for biological ^{31}P NMR spectroscopy. The international standard for ^{31}P chemical shift was, and still is, 85% phosphoric acid in $^{2}H_2O$; perforce, it is an 'external' reference that must be housed in a glass capillary, or spherical bulb, inserted into the sample and thus isolated from the (bio)molecules of interest. The use of this standard has significant shortcomings in the context of cell suspensions, in which, as is described below, variations in magnetic susceptibility between the contents of the reference-capillary and the cells can contribute to apparent chemical shift differences seen in the NMR spectra.

Endogenous metabolites can be used as 'internal' chemical shift references in some tissues, such as phosphocreatine in muscle. This has a value of -2.3 ppm at pH 7.42, but it is calibrated relative to external 85% phosphoric acid in $^{2}H_2O$ [9], which we considered to be non-ideal for reasons stated above; furthermore, phosphocreatine is not present in human RBCs.

Amongst a group of candidates for internal reference compounds, the water-miscible, electrically neutral ester, dimethyl methylphosphonate (Fig. 1A, DMMP) was appealing. Its single ^{31}P atom is surrounded by three oxygen atoms, with a directly bonded carbon atom that defines it as a phosphonate. It was expected to give a single ^{31}P NMR resonance with a chemical shift to high frequency of the resonances from endogenous phosphate esters, thus avoiding spectral resonance overlap with them. However, when DMMP was added to freshly prepared human RBCs, the ^{31}P NMR spectrum contained not the expected single resonance, but two! This was the foundational serendipitous discovery.

We set out to understand the physicochemical origins of this phenomenon, and to explore how it could be used to probe various properties of RBCs.

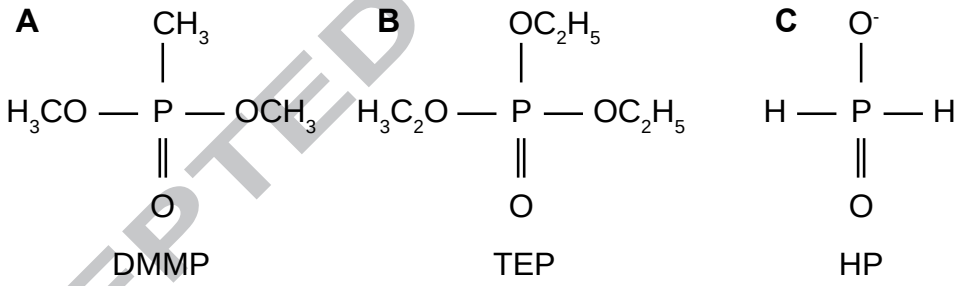

Fig. 1 Three phosphoryl compounds that were important in the development of ^{31}P NMR methodology that emerged from the study of the split peak effect. **A**, Dimethyl methylphosphonate (DMMP) shows separate intra- and extracellular ^{31}P NMR resonances when added to a cell suspension and has been used for measuring changes in cell volume [2] and membrane permeability on the sub-second time scale [10]. **B**, Triethyl phosphate (TEP) is the ^{31}P NMR chemical-shift and intensity reference for general use in cell suspensions [11]; it undergoes fast-exchange across the erythrocyte membrane under physiological conditions and gives rise to a single ^{31}P NMR resonance. **C**, Hypophosphite (HP), like DMMP, shows the split peak effect and is used for measuring membrane potential [12], as an analogue of bicarbonate in membrane transport studies, and to record changes in cell volume during time courses in which other cell attributes are recorded [13].

Further experiments revealed more intriguing characteristics of the ^{31}P NMR signals from DMMP. Fig. 2A shows the separation between the two peaks of DMMP and how this increased with a decrease in mean cell volume (MCV), brought about by changing the

osmolality of the medium by changing the NaCl concentration [2]. This spectral series also served to identify the low chemical shift resonance as being from the intracellular population of DMMP molecules. The osmotic shrinking reduced the RBC water volume while increasing that of the extracellular compartment. Hence the peak with the decreasing integral (area) can be deduced to be from DMMP inside the cells, while the increasing one is from DMMP outside them. In other words, it was the low chemical shift peak (to the right in the spectra of Fig. 2A) for which the integral changed in this way, thus identifying it as being from the intracellular DMMP. The observation that the low chemical shift resonance moved to a greater extent than the high chemical shift one, as the cell volume was varied, underscored the conclusion that this resonance was indeed from DMMP inside the cells.

Fig. 2B is a graph of the dependence of the DMMP resonance separation on the RBC volume (MCV), measured using the initial cell count and a standard haematological procedure to measure the haematocrit (*Ht*) with a special centrifuge. This outcome was important as it provided a tool for real-time monitoring of MCV. Once a blood sample from a particular donor has been calibrated with respect to DMMP splitting as a function of RBC volume, changes in MCV during time course experiments can be monitored in a quantitative manner by referring the resonance separation back to the standard line.

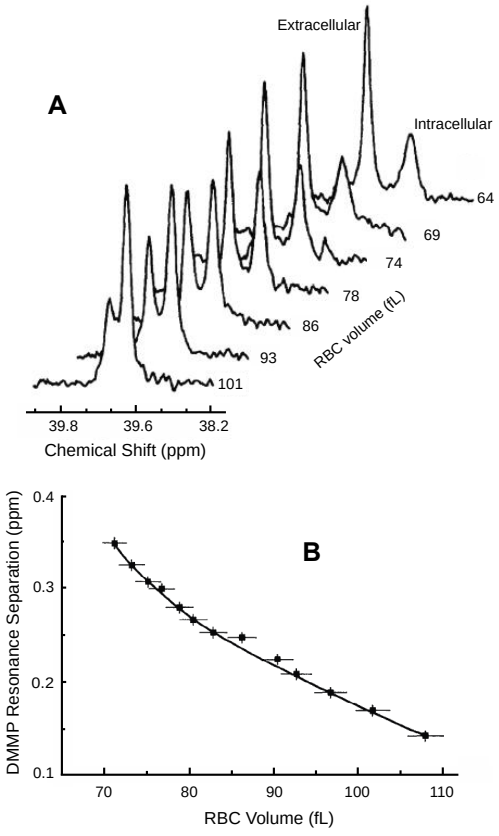

Fig. 2 ^{1}H-decoupled ^{31}P (162 MHz) NMR spectra of DMMP in a suspension of RBCs with a progressive decrease in RBC volume brought about by adding concentrated NaCl solution to a previously hypotonic medium. **A**, Chemical shift separation between the two resonances (peak splitting) increased as the RBC volume was decreased; the resonances that corresponds to the respective extracellular and intracellular populations of DMMP are labelled in the top spectrum . **B**, Graph of resonance separation (peak splitting) as a function of RBC volume. Adapted from the original [2], with permission of Elsevier.

3. Possible mechanisms

3.1. pH and binding

In subsequent work, the separation of the DMMP resonances in RBC suspensions was seen to change with changes in pH; however this was soon shown to be an indirect effect, secondary to the influence of pH on the MCV [14]. The ^{31}P NMR chemical shift of DMMP (a non-ionisable, electroneutral compound) itself is independent of pH.

When the packing density of the RBC sample (the *Ht*) was varied by adding more packed cells to an existing sample, the resonance separation remained almost constant. Additionally, the magnitude of the splitting was independent of the concentration of DMMP up to bio-tolerable concentrations (~50 mM). Both of these results argued against tight (saturable) binding to haemoglobin (or other less abundant proteins and lipids) as the basis for the chemical shift of the intracellular resonance.

In experiments with haemolysates, it was shown that the frequency of the ^{31}P NMR signal from DMMP, relative to that of triethyl phosphate (a compound shown to have a ^{31}P NMR signal that made it ideally suited for use as an internal chemical-shift standard; see below and Fig. 1B for its structure), was dependent mostly on the haemoglobin concentration [14, 15].

In summary, it appeared from the early work with DMMP that its split peak effect was not due to direct saturable binding to macromolecules in RBCs, and yet it was dependent on the protein (mostly haemoglobin) concentration.

3.2. Other phosphonates

Following the original observation of the DMMP split peak effect, a set of other phosphoryl compounds was added to RBC suspensions (Fig. 3A). With the exception of triethyl phosphate (TEP), all showed the split peak effect. The compounds for which peak

splitting was seen included the charged monovalent hypophosphite anion (HP; Fig. 1C), while the remainder were electroneutral esters like DMMP. For those compounds showing the split peak effect, there was a high degree of variability in the magnitude of the separation between the intra- and extracellular resonances. For isovolumic RBCs (MCV = 86 fL), the largest splitting was seen with diphenylphosphinate (DPP; 1.324 ppm) and the smallest splitting was with trimethyl phosphate (TMP; 0.055 ppm).

Fig. 3B shows the effect on the NMR spectrum of Fig. 3A, obtained by adding 100 µM $MnCl_2$ to the RBC suspension. The extracellular Mn^{2+} causes suppression and broadening of the higher frequency (higher chemical shift) component of the split peak, thus confirming the identity of this resonance as the extracellular one. Note that in the case of the anionic species phenylphosphinate (PP) and hypophospite (HP), addition of $MnCl_2$ resulted in the complete elimination of the extracellular resonance (Fig. 3B).

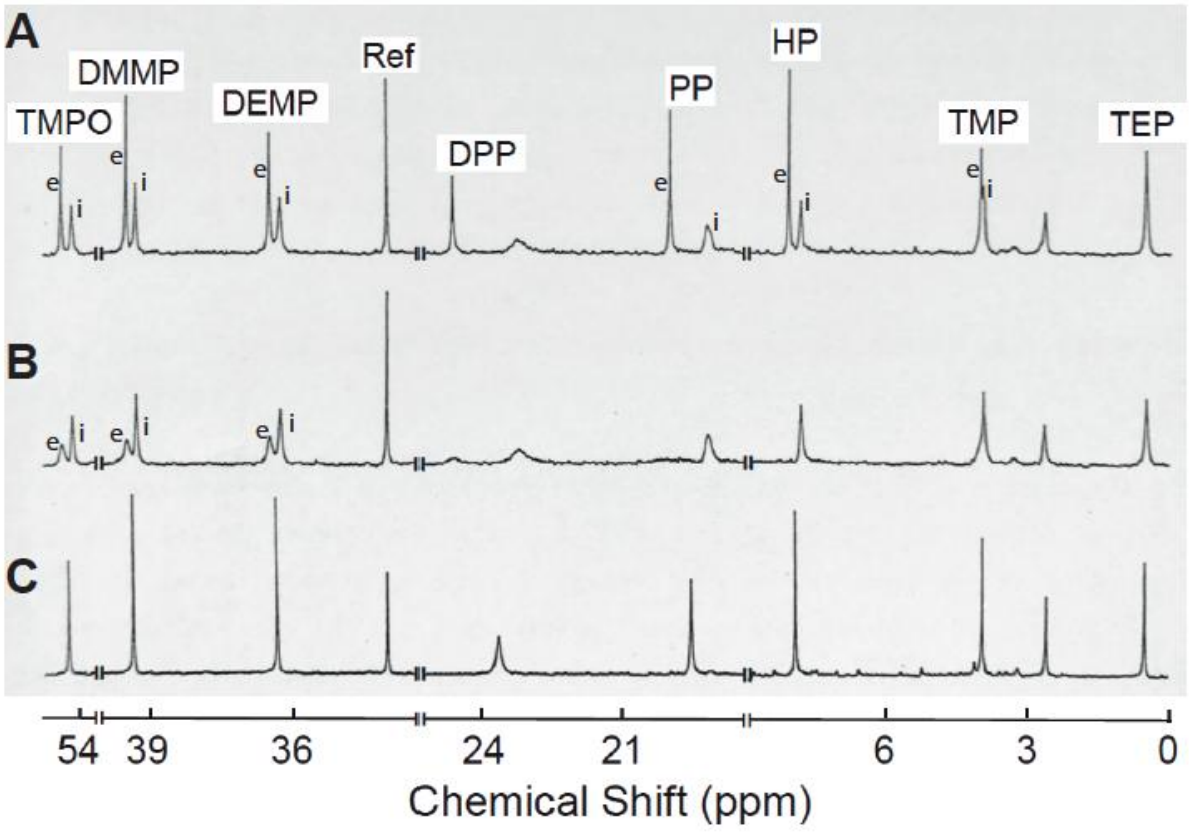

Fig. 3. ^{1}H-decoupled ^{31}P (162 MHz) NMR spectra of eight phosphoryl compounds, each at a concentration of 10 mM, in an RBC suspension that had been treated with carbon monoxide to convert the haemoglobin to its stable diamagnetic (carbonmonoxy) state. **A**, An RBC suspension with *Ht* = 0.56, where e and i denote extracellular and intracellular resonances, respectively. **B**, A similar suspension to which 100 µM $MnCl_2$ was added. **C**, A haemolysate prepared by freeze-thawing of a suspension of RBCs prepared as for **A**. Abbreviations

and peak separations (ppm) at an RBC volume of 86 fL: trimethylphosphine oxide (TMPO), 0.212; dimethyl methylphosphonate (DMMP), 0.195; diethyl methylphosphonate (DEMP), 0.209; diphenylphosphinate (DPP), 1.324; phenylphosphinate (PP), 0.316; hypophosphite (HP), 0.233; trimethyl phosphate (TMP), 0.055; triethyl phosphate (TEP), 0.000; and 'Ref' indicates the peak of DEMP in a glass capillary serving as an external (secondary) chemical shift standard. Resonances at 3.42 and 4.17 ppm were from 2,3BPG in the RBCs, while a signal from intracellular inorganic phosphate was at 2.78 ppm. Adapted, using the original spectra from Fig. 3.1 in [16], with new solid lines and symbols. A version of the figure with only the top spectrum is Fig. 1 in [17]. Adapted, with permission of Elsevier.

3.3. Magnetic susceptibility differences

One potential source of a chemical shift difference between intra- and extracellular populations of the compounds of interest is a difference in magnetic field strength between the inside of the RBCs and the medium. This can be brought about by differences in magnetic susceptibility of the intra- and extracellular milieux. If the local magnetic field is different inside and outside the cells, the Larmor equation (Eq. 1) predicts different resonance frequencies for corresponding nuclei (in a particular molecule) located in the two compartments.

It is sometimes forgotten that haemoglobin is not always paramagnetic. In fact, the globin, and porphyrin parts of the heme moiety, are diamagnetic [18, 19]. The iron in heme can exist in several different electronic states. The Fe(II) state is only paramagnetic when *no* oxygen is bound to it: in deoxyhaemoglobin, Fe(II) exists in a high-spin electronic state and, as a result, it is paramagnetic. In methaemoglobin, the iron exists in the paramagnetic Fe(III) state, rendering the protein as a whole paramagnetic. However, oxy- and carbonmonoxy-haemoglobin are both diamagnetic [18]. It is with this in mind that, in order to achieve the highest resolution in NMR spectra, RBC suspensions are often gassed with carbon monoxide to lock haemoglobin into the low-spin diamagnetic (carbonmonoxy-haemoglobin) state. Because the affinity of haemoglobin for carbon monoxide is ~250 times that for oxygen [20], the sample remains diamagnetic for many hours in a sealed NMR tube. This high affinity is highlighted by the observation that the biological half-life of carbon monoxide in a healthy sedentary adult is 4-5 h [20]; this is something worth remembering when using this gas to prepare blood samples in experimental studies.

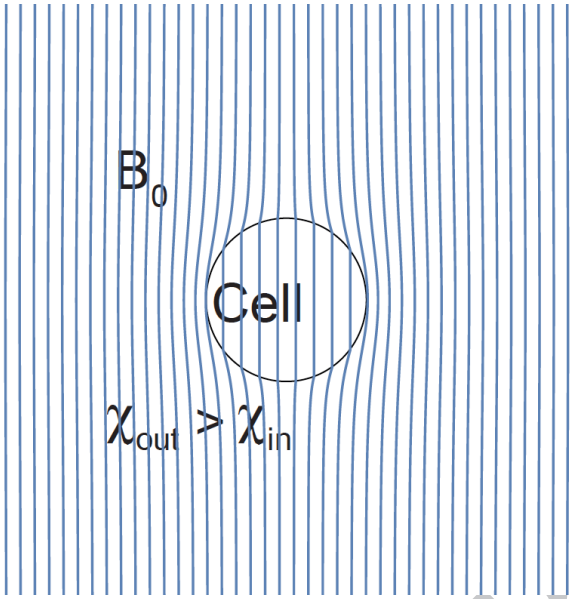

Fig. 4. Representation of magnetic field distortion by a spherical cell enclosing a medium that has lower magnetic susceptibility, χ_i, than that in the extracellular medium, χ_e. The cell is typically more diamagnetic than the surrounding medium as is the case of oxygenation or carbon-monoxygenation of RBCs. The separation or distance between the lines of force indicates the relative magnetic induction, or flux density, in the depicted region. The figure is based on a solution of the Laplace equation using *Mathematica* [21] for which χ_i: χ_e = 1:1.9.

Fig. 4 represents a physical situation that may seem intuitively obvious: if the interior of a cell is more diamagnetic than outside, then the bulk magnetic field strength inside will be less than that outside. While there are gradients of the field near the outer surface of the sphere, the field inside is homogeneous. It could be surmised from Eq. (1) that, providing that transmembrane exchange is slow on the NMR time scale, the net effect of this situation will be separate NMR peaks arising from the solute nuclei inside and outside the cells. Because the field outside the cell is not homogeneous, the spectral lines from nuclei in the immediate vicinity of the cell will be broader than those from nuclei inside the cell, or in the bulk external phase because of the range of magnetic field strengths.

However, the situation is not this simple. Cells, and the medium in which they are suspended, are magnetically polarized by the imposed magnetic field, $\mathbf{B}_0$. This polarisation of the contents of each compartment makes a contribution to the magnetic field that is experienced by nuclei within that compartment. This contribution combines with the magnetic field arising from induced magnetic dipoles from adjacent nuclei which averages to

zero in an isotropic system, but not necessarily so in complex structures like the inside of a cell.

While we will not digress into this topic here, it can be shown that for an isolated sphere in a uniform imposed magnetic field, the field experienced by a nucleus within the sphere is the same as that experienced by a nucleus in the same solute species in the external medium. This is why a 'true' external chemical shift standard is placed into a glass sphere inside the NMR sample tube. On the other hand, cells in a dense suspension cannot be assumed to be spherical (RBCs certainly are not under normal circumstances) or isolated from each other, so the inside magnetic field is also not homogeneous. As a general rule of thumb, if the cellular contents are more diamagnetic (less paramagnetic) than the external medium, then resonance frequencies will be lower inside the cells than their counterparts outside. The subject of magnetic susceptibility-induced resonance shifts is comprehensively covered in references 22-24 [22-24] and an illustration of the effect is presented below under the heading "***Differential hydrogen bonding of water inside and outside RBCs*** ".

Overall, in the absence of other factors, such as specific chemical interactions, the extent of peak splitting arising from a transmembrane magnetic susceptibility difference will be the same for the nuclei in all solutes. The data in Fig. 3 clearly show this not to be the case. So, if a magnetic susceptibility difference did contribute to the splitting of the peaks, it could not the sole cause.

3.4. Solvent effects

Earlier studies by Natterstad and Maciel provided the key to our understanding of a likely cause of the split peak effect [25-27]. They explored solvent effects on the chemical shift in ^{13}C NMR spectra of a series of eight carbonyl compounds, including acetone. The chemical shift of the ^{13}C=O group was measured in samples made in 17 different solvents ranging from aprotic ones (including acetone itself, cyclohexane, and methanol) to protic solvents (including acetic acid and 97% sulfuric acid in water). The solvent series was ranked in terms of the tendency to form hydrogen bonds between the solvent and solute molecules. The full range of ^{13}C chemical shifts of ^{13}C-acetone was a mighty 43.6 ppm (not including neat acetone itself). In the same solvents, the range of shifts of ^{13}C-dimethyl carbonate was only 3 ppm (not including sulfuric acid as the solvent) suggesting the use of this compound as a general internal ^{13}C NMR chemical shift reference [27]. The near invariance of the difference in chemical shift between its methyl and carbonyl resonances also had a bearing on the

mechanism deduced for the solvent shift effect seen with the other solutes. This observation prompted the idea of finding an analogous compound as an internal chemical shift standard for our ^{31}P NMR studies. TEP turned out to be the best candidate [11] (see Fig. 3, and below).

The study of solvent effects on the ^{13}C NMR chemical shifts of compounds containing the carbonyl group led us to explore whether the ^{31}P NMR chemical shifts of the various phosphoryl compounds of interest showed analogous solvent dependence. A range of solvents were tested: heptane, cyclohexane, benzene, carbon tetrachloride, acetone, chloroform, *tert*-butyl alcohol, isobutyl alcohol, 2-propanol, 1-pentanol, 1-butanol, 1-propanol, ethanol, methanol, water, $^{2}H_2O$, acetic acid, and sulfuric acid. The chemical shift of DMMP spanned from -7.3 to 11.1 ppm, *viz.*, over 18 ppm! DEMP and TMPO showed similarly large chemical shift ranges, while TEP had a chemical shift range of only 0.5 ppm [28]. This property, coupled with its metabolic inertness, made (and still makes) TEP an ideal internal chemical shift reference for ^{31}P bio-NMR [11].

When interpreting the chemical shift behaviour of the different phosphoryl compounds dissolved in the different solvents, it was recognized that the solvents varied in the extent to which they participate in hydrogen bonding with each of the compounds (as in [27]). For the two phosphate esters (TEP and TMP), the variation in hydrogen bonding at the phosphoryl oxygen was evidently of little consequence for the ^{31}P NMR chemical shifts. Having the carbon atom directly bonded to the phosphorus atom in the phosphonates was clearly important for the solvent-shift effect. In rationalizing the physicochemical features of this solvent set, the feature that correlated with the observed chemical shift of DMMP (as well as those of DEMP and TMPO) was the extent to which each solvent is able to participate in hydrogen bonding, primarily as a donor to the phosphoryl oxygen. This led to the hypothesis that the observation of separate intra- and extracellular peaks for many of the phosphoryl compounds in a suspension of RBCs reflects, at least in part, a difference in the extent of hydrogen bonding, primarily to water (since this is by far the most abundant hydrogen bond donor in the system), inside and outside the cells. It was postulated that because of the high concentration of protein within RBCs, the extent of hydrogen bonding between the probe compounds and water will be lower inside the cells relative to the suspension medium outside the cells.

This hypothesis for the primary mechanism underlying the split peak effect led us to postulate that the effect would also be seen with fluorinated compounds. Although controversial [29], it had been claimed by various authors that the fluorine atom can act a

hydrogen-bond acceptor in some compounds, and this now appears to be well accepted [30]. Thus, a different hydrogen bonding environment to water inside and outside the cells might be expected to give rise to differences in the ^{19}F NMR chemical shifts of intra- and extracellular populations of fluorinated compounds, as had indeed been observed.

4. ^{19}F NMR spectroscopy of RBCs

4.1. Previous interpretations

London and Gabel [31] had observed split peaks in ^{19}F NMR spectra of trifluoroacetamide and trifluoroacetate added to RBC suspensions. They used the phenomenon to measure the membrane potential in a manner that was similar to our use of HP with ^{31}P NMR (see below). However, they ascribed the ^{19}F NMR spectral splitting to differences in magnetic susceptibility between the inside and outside of the cells, in addition to differential binding to cellular constituents. The latter idea was invoked to account for the observation that the separation between the intra- and extracellular peaks was different for the two compounds; as noted above, a magnetic susceptibility difference alone would have given the same split for both compounds.

4.2. 3-Fluoro-3-deoxy-D-glucose

A clear difference between the splitting observed with ^{31}P and ^{19}F compounds is the *direction* of the intracellular shift. As can be seen from Fig. 5, on adding 3-fluoro-3-deoxy-D-glucose (FDG-3) to a suspension of RBCs [32, 33], the resonance from the intracellular population of this glucose analogue is to high chemical shift of the extracellular one. This is the opposite of what is seen in the ^{31}P NMR spectra of phosphoryl compounds added to RBC suspensions (*e.g.*, Figs 2A and 3).

This observation argues against the phenomena being simply due to differences in magnetic susceptibility across the cell membrane. The effect is particularly well exemplified in the spectra from a molecule with two different NMR-receptive nuclides in its structure, difluorophosphate (DFP, F_2-(P=O)-(O^-)$_2$).

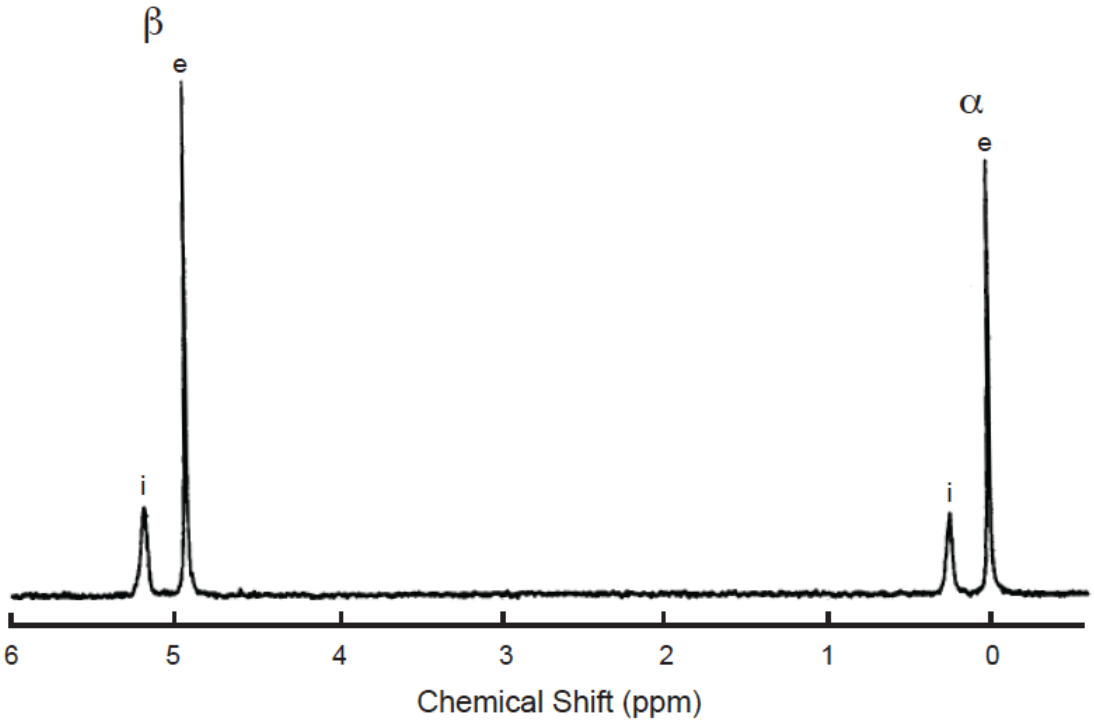

Fig. 5. ^{1}H-decoupled ^{19}F (376 MHz) NMR spectrum of 3-fluoro-3-deoxy-D-glucose added to a suspension of RBCs. Annotation: α and β denote the resonances from the respective anomeric species, while e and i denote the extracellular and intracellular resonances, respectively. The chemical shift of the extracellular resonance of the α-anomer was set to 0.000 ppm. Adapted, with permission of Portland Press, from [33].

4.3. Difluorophosphate – the "clinching" evidence

Fig. 6A shows a ^{31}P NMR spectrum of DFP in a RBC suspension, with its widely-dispersed triplet showing a ^{19}F-^{13}P scalar coupling of $^{1}J_{FP}$ = 975 Hz. In addition, each component of the triplet is split into intracellular and extracellular peaks. The signals arising from the intracellular population are to lower frequency. Fig. 6B shows the ^{19}F NMR spectrum of DFP, with a doublet of the same splitting (975 Hz), as would be expected from the $^{1}J_{FP}$ value seen in the ^{31}P NMR spectrum. The important difference between the spectra of Figs 6A and 6B is that the intracellular shift in the opposite direction.

The simplest explanation (invoking Occam's razor) for these spectral outcomes is that the split peak effect arises from there being different extents of hydrogen-bonding of the solute of interest to water, inside and outside the cells. As alluded to above, this is most likely due to the high content of proteins (mostly haemoglobin) inside the RBCs and hence effectively reduced extent of interactions between the solute of interest and water. Both the phosphoryl

oxygen and the fluorine atom participate in hydrogen bonding with water. For the ^{19}F atom, the hydrogen bond is directly to the NMR reporter nucleus, whereas for the ^{31}P spectrum, the chemical-shift perturbation takes place inductively via the intervening oxygen atom in the phosphoryl group [34]. As a result, the intracellular shifts, observed for the two nuclei, are in opposite directions.

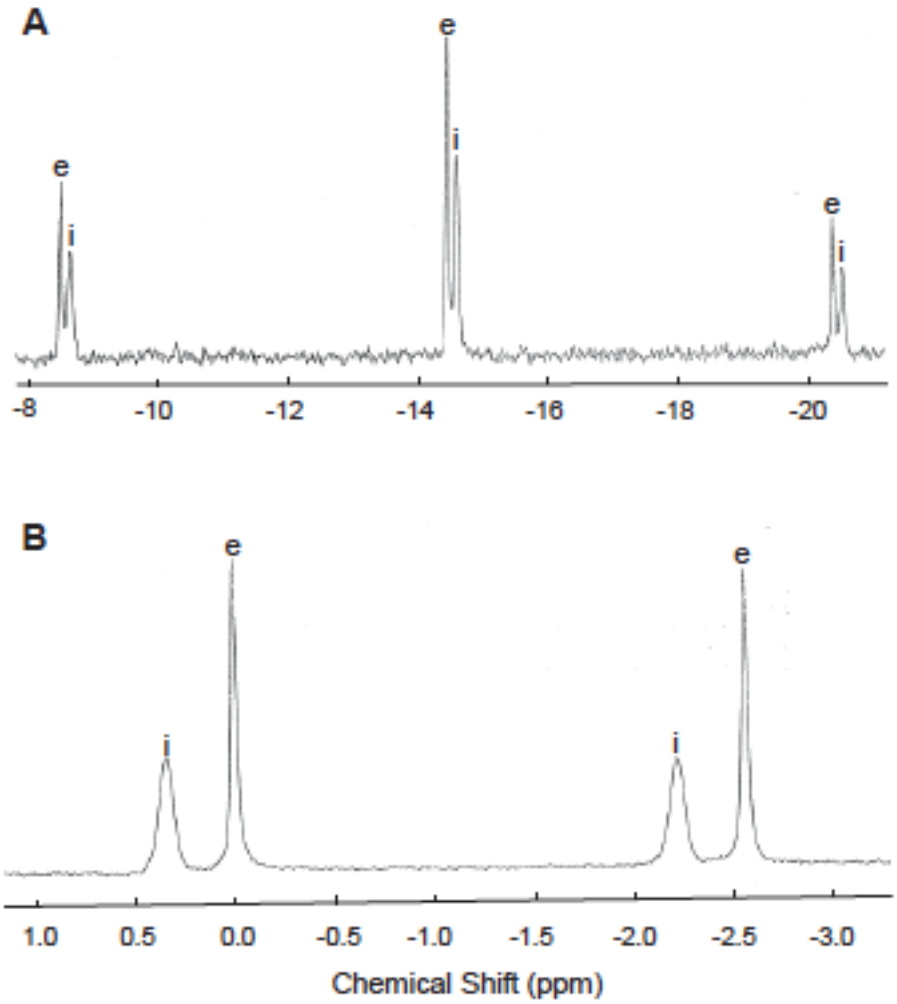

Fig. 6. NMR spectra of difluorophosphate (DFP) in a suspension of RBCs. **A**, ^{31}P (162 MHz) NMR spectrum; **B**, ^{19}F (376 MHz) NMR spectrum. The extracellular and intracellular resonances are denoted with e and i, respectively. Adapted, with permission of Wiley, from [34].

The notion of different extents of hydrogen bonding in the intra- and extracellular compartments raises the question of whether water itself might undergo different extents of hydrogen bonding inside and outside RBCs. The answer to this question was provided by using ^{1}H NMR spectroscopy, but with a twist, as is described next.

5. Differential hydrogen bonding of water inside and outside RBCs

5.1. Variable angle spinning and magic angle spinning

Water exchange across the RBC membrane, mediated by aquaporin 1, is fast on the NMR time scale. Thus, only one resonance at a weighted-average chemical shift of ~4.8 ppm is typically observed in ^{1}H NMR spectra of RBCs [35]. However, by using a variable-angle spinning (VAS) NMR probe with a cylindrical rotor, effectively serving as a mini-centrifuge, it is possible to resolve the intra- and extracellular resonances. The RBCs are denser than water and are therefore pelleted to the walls of the cylinder, away from the extracellular solution. Under these conditions, the ^{1}H NMR spectrum shows separate resonances from intra- and extracellular water (Fig. 7) [36].

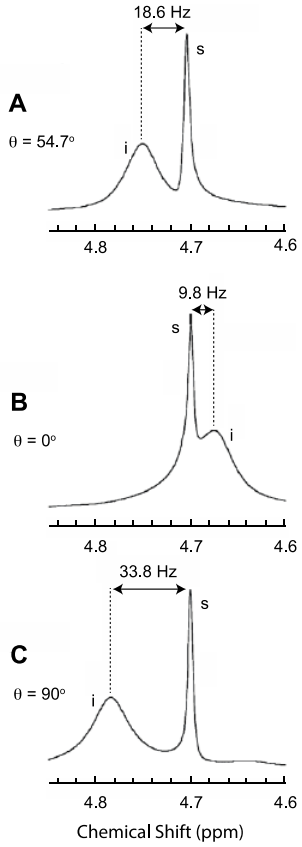

Fig. 7. ^{1}H (400 MHz) NMR spectra of water in an RBC suspension of *Ht* = 81% at 37°C in a VAS rotor spun at 250 Hz. **A**, The spinning axis of the rotor θ was the magic angle 54.7°; **B**, 0°; and **C**, 90°. Separations between

the maxima of the intracellular (i) and supernatant peaks (s) are indicated by arrows. Original high chemical shift sections of the spectra were taken from Fig. 1 of [36]. With permission from Wiley.

The two resonances are (partially) resolved because exchange between the intra- and extracellular water populations is largely eliminated by the physical separation of the two populations. Effectively, transmembrane water exchange only takes place between the supernatant solution in the centre of the rotor and the relatively few cells at the interface with this solution; the majority of the RBCs only exchange water amongst themselves via the small fraction of water in the interstitial space. Because there was no change in the chemical shift of the resonance of the intracellular water with a change in angular velocity from 250 Hz to 7 kHz we concluded that the insterstitial water space (which might be expected to be decreased at the higher angular velocity) was insignificant.

Thus, the split peak effect that might be predicted to occur on the basis of hydrogen-bonding considerations can be observed directly from the ^{1}H NMR spectra of water acquired under the conditions of the VAS experiment [36]. Under the special condition of a spinning VAS rotor orientated at the magic angle (54.7^{o}), bulk magnetic susceptibility effects are negated [37, 38]. So, what is evident in the spectrum of Fig. 7A is a true isotropic chemical shift difference between the intra- and extracellular populations of water *without* a contribution from the bulk magnetic susceptibility difference of the two compartments. Thus, the resonance splitting is identified as being due to two physico-chemically different water environments [36, 39].

When the rotor was aligned with its long axis in the direction of $\mathbf{B}_0$, the peak from intracellular water was to low frequency of that from the supernatant (Fig. 7B). This identified the interior of the RBCs as more diamagnetic (more negative magnetic susceptibility) than outside in the supernatant. This is the well-defined property of oxy- and carbonmonoxyhaemoglobin, discussed above [19]. When the rotor was spun with its long axis at 90^{o} to $\mathbf{B}_0$, the peak from the intracellular water moved to higher frequency of that from the supernatant. While this outcome is perhaps surprising, it is exactly as predicted [22, 40] for a coaxial cylindrical sample in which the magnetic susceptibility of the extracellular solution is higher than that of the cell interior. We also recall that the diamagnetic character of oxyhaemoglobin affected the value of the chemical shift of the ^{31}P NMR resonance of TEP, and other phosphoryl compounds, in haemolysates [41].

5.2. Magnetic susceptibility measurement

Quantitative information about the *magnitude* of the magnetic-susceptibility-induced difference between the RBCs and the supernatant can be extracted from the spectra obtained by spinning the rotor at 54.7^o (Fig. 7A), 0^o (Fig. 7B), and 90^o (Fig. 7C), relative to $\mathbf{B}_0$. The requisite theory to analyze the data corrected previous conclusions [42], in which the 'sphere of Lorentz correction' had not been applied, and therefore the peak splitting at the magic angle was wrongly ascribed to an "isotropic bulk magnetic susceptibility shift" [42]. To confuse the matter further, earlier work had attributed the splitting of the water resonance to removal of dipolar broadening of intracellular and interstitial water by spinning at the magic angle, and did not ascribe it to the effect of centrifugation of the RBCs away from a supernatant in the spinning rotor [43]. The conclusion that water resonance splitting in RBCs, spun at the magic angle, is due to an altered water environment inside was subsequently settled upon, and also extended to selected cultured cells [39].

5.3. *Peak splitting - a combined effect*

The analysis of the physical phenomena behind the split peak effect of the water resonance in RBC suspensions led to the conclusions that the separation of the intra- and extracellular peaks is due to a combination of an isotropic effect or chemical interaction (that is uniform throughout the sample and has no variation with sample orientation), and magnetic susceptibility differences between the intra- and extracellular compartments [36]. Therefore, the hypothesized hydrogen-bond-induced split peak effect was observable directly in the ^{1}H NMR spectrum of water in RBCs, under the special conditions of a VAS, or magic angle spinning (MAS), rotor [36]. It is a remarkable observation (different chemical activity of water in cells) that would be difficult to make by any method other than VAS and/or MAS NMR.

6. Selected applications of the NMR split peak effect

6.1. General

Any method for measuring the exchange of molecules or inorganic ions across cell membranes requires either a physical or chemical means of distinguishing the intra- and

extracellular compartments from one another. In its simplest form, a membrane transport assay for a solute can entail physically separating the cells from the extracellular solution by centrifugal sedimentation, or filtration. In such assays, the amount of solute inside the cell is typically measured after rupturing the cells and extracting the contents. The amount of solute in the extracellular solution may also be measured. This approach often involves incorporating a radioactive label into the solute of interest, or the use of specific detectors such as ion-selective electrodes, high-performance liquid chromatography, or mass spectrometry. Methods that entail the preparation of cell extracts are, by definition, invasive. There are obvious benefits associated with the use of non-invasive methods; *e.g.*, the possibility of simultaneous monitoring of other cellular attributes, such as pH, metabolic activity, redox status, and even cell volume and shape. NMR spectroscopy provides such capability by exploiting differences in various NMR characteristics that arise naturally (or can be imposed) between the inside and outside of cells [44-46]. Such properties include differences in: (1) longitudinal and transverse relaxation times: T_1 [47], T_2 [48, 49], and T_2* [50]; (2) scalar, *J*, coupling constants [51]; (3) chemical shifts of atomic nuclei in molecules that rapidly bind and exchange H^+ or metal ions [52, 53]; (4) extents of restricted diffusion [54-56]; (5) rates of chemical exchange between species in each compartment [57, 58]; and (6) as considered in this review, the extent of hydrogen bonding undergone by solutes that have an NMR-receptive reporter nucleus.

6.2. ^{31}P NMR

As discussed above, the first molecule for which the split peak effect was demonstrated was DMMP. The phenomenon was used to monitor changes in the MCV [2], and in the first application of an NMR magnetization-transfer technique to estimate the rapid (sub-second) exchange rate of a solute across a cell membrane [10].

The ^{31}P NMR split peak of hypophosphite (HP) was used for probing the membrane potential [12] and the transport properties of the Band 3 anion-exchange protein of the RBC [59]. The intra- and extracellular ^{31}P NMR peaks of HP are sufficiently well resolved to allow the estimation of the relative quantities of the anion inside and outside the cells simply by peak integration; and this enables calculation of the corresponding concentrations and hence estimation of the membrane potential via the Nernst equation. The transmembrane transport rates of compounds such as DMMP and HP can measured by NMR diffusion-measuring [59] and magnetization-transfer experiments, as has been recently reviewed [60].

6.3. ^{13}C NMR

The split peak effect was observed in ^{13}C NMR spectra of [1-^{13}C]- and [2-^{13}C]ascorbic acid, and was used to monitor the transport and redox cycling of the compounds across the RBC membrane [61]. The ^{13}C-urea resonances from inside and outside RBCs are partially resolved from one another [62] and this can be used for estimating the values of the kinetic parameters that characterize urea exchange across the RBC membrane under equilibrium exchange conditions [62] and non-equlibrium (zero-trans) conditions (*i.e.*, when the solute is absent from the opposite 'trans' side of the membrane) [63]. In the context of using NMR spectroscopy to study membrane transport under zero-trans conditions, recent experiments exploited the new rapid-dissolution dynamic nuclear polarization technology (RD-DNP) to achieve this [64].

^{13}C-Formate shows the split peak effect with RBCs, but as for urea, the two peaks are not fully resolved in a magnetic field of 9.4 T. Nevertheless, saturation-transfer spectra acquired in the presence and absence of 4 ,4'-dinitrostilbene-2,2'-disulfonic acid (DNDS), an inhibitor of the Band 3 anion exchange protein, were suitable for producing initial estimates of the exchange rate constants on the sub-second time scale [65]. Because of the peak overlap, alternative methods (that do not rely on full separation between the two peaks for the analysis) were used to obtain more accurate estimates of these rate constants. Specifically, we performed kinetic analyses based on differences in T_1 value between the intra- and extracellular compartments, after addition of Mn^{2+} to the medium. We also used NMR diffusion measurements in this system, since the apparent diffusion coefficients of ^{13}C-formate differ significantly between the inside and outside of RBCs. The latter property enabled the application of Kärger's two-site exchange analysis [56, 66, 67] that confirmed the rapidity of formate exchange via the Band 3 protein [68].

6.4. ^{133}Cs NMR

Caesium cation, a congener of the potassium cation, has several distinctive NMR properties, combining a high natural abundance (100% for ^{133}Cs), a high NMR receptivity (some 10-fold higher than that of ^{39}K) and a large chemical shift range with relatively narrow linewidths (due to a small quadrupole moment). Cs^+ enters cells via endogenous K^+ transport pathways, especially the Na^+,K^+-ATPase, and shows a split peak effect. The Cs^+ ion is

hydrated, and it is this molecular ion that interacts with bulk water. Although it has not been investigated in detail, it is plausible that the split peak seen for Cs^+ is based on the different extents of hydrogen bonding of the molecular ion to bulk water inside and outside cells. These beneficial NMR properties allowed the use of ^{133}Cs NMR to study the distribution of $^{133}Cs^+$ in various rat tissues [69] and even between different intracellular compartments in rat hepatocytes [70].

In RBCs, ^{133}Cs NMR spectroscopy has been used to probe the intracellular environment relative to a suspension medium containing a high concentration of gelatin gel; the concentration of the latter can be comparable to that of haemoglobin inside the RBCs. Stretching or compressing the sample partially aligns the molecules of denatured collagen, of which gelatin is composed. For $^{133}Cs^+$ in the (extracellular) stretched or compressed gel, its resonance is split into a septet as a result of the partial molecular alignment causing residual quadrupolar coupling with the $^{133}Cs^+$ nucleus (spin quantum number of $^{133}Cs^+$ is 7/2) [71]. By contrast, the intracellular $^{133}Cs^+$ resonance remains a singlet. Thus, it was concluded that, despite the cells undergoing visible distortion under the stretched/compressed conditions [72], the intracellular environment (dominated by haemoglobin and the sub-membranous cytoskeleton) is not ordered in the same way or to the same extent as the aligned gel outside [71].

6.5. ^{19}F NMR

The first report of a split peak effect in ^{19}F NMR spectra of cells was for trifluoroacetate and trifluoroacetamide added to a RBC suspension [31]. These compounds were used to measure the membrane potential and the MCV of RBCs [31]. As noted above, the authors ascribed the peak splitting to a magnetic susceptibility difference between the inside and outside the cells, combined with binding to macromolecules. The reduced values of T_1 and T_2 relaxation times of the intracellular species were presented as evidence of putative intracellular binding/exchange reactions.

Our first application of the ^{19}F-NMR split peak effect for measuring membrane transport was with 3-fluoro-3-deoxy-D-glucose (FDG-3), used as a probe-substrate for the erythrocyte glucose transporter, GLUT1. In initial experiments, the saturation-transfer method was used to estimate transmembrane exchange rate constants [32], and this was followed more comprehensively with overdetermined 1D-EXSY methodology [33].

London et al. used 1D- and 2D-EXSY methods to study differences in the rate of transmembrane transport of the α- and β-anomers of several monofluorinated analogues of glucose, labelled with an F-atom at various positions; *viz.*, 2-fluoro-2-deoxy-D-glucose (FDG-2), FDG-3, 4-fluoro-4-deoxy-D-glucose (FDG-4) and 6-fluoro-6-deoxy-D-glucose (FDG-6) [73], as well as glucosyl fluoride (1-fluoro-1-deoxy-D-glucose, FDG-1) [74]. These studies led to a proposal for a molecular mechanism of the operation of the active site of GLUT1 transporter [74].

Recently, Dickinson et al. measured the transport of FDG-3 in RBCs to investigate changes in membrane permeability of RBCs from pregnant women with preeclampsia [75]. They concluded that there were no significant differences between the RBCs from the patients and those from a control group; the changes in glucose transport that are reported to occur in vascular endothelia are evidently not expressed in RBCs.

2D-EXSY methodology has also been applied in membrane-transport studies of *poly*fluorinated sugars: 2,2,3,3,4,4-hexafluoro-2,3,4-trideoxy-D-glucose (FDG-223344) [76] and 2,3,4-trifluoro-2,3,4-trideoxy-D-glucose (FDG-234) [77]. The ^{19}F-NMR spectra of FDG-234 clearly show the split-peak effect, and the 2D-EXSY transmembrane-exchange peaks are presented in Fig. 8. Both studies demonstrated that these compounds are transported rapidly across the RBC membrane. The transport of polyfluorinated sugar presumably occurs via GLUT1, but this has not been investigated in detail.

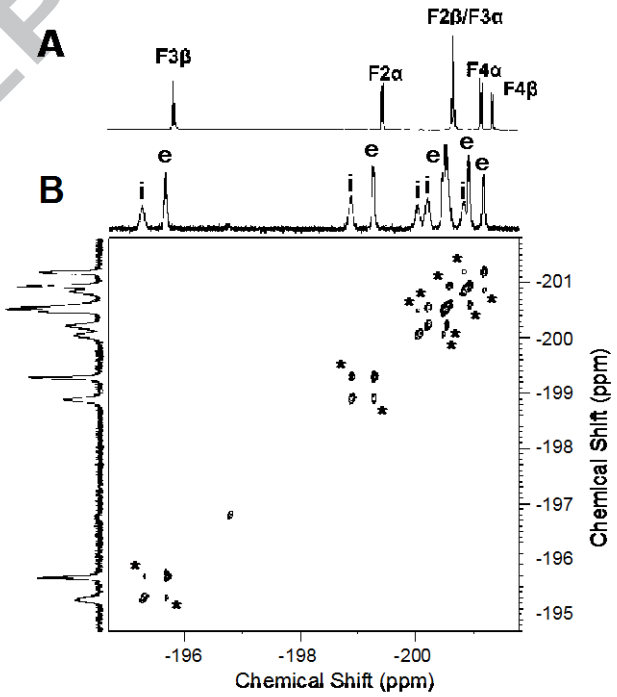

Fig. 8. ^{1}H-decoupled ^{19}F (470.4 MHz) NMR spectra of 2,3,4-trifluoro-2,3,4-trideoxy-D-glucose (FDG-234) at 37ºC. **A**, 1D spectrum of FDG-234 in 123 mM NaCl, 15 mM Tris/HEPES, 5 mM ascorbate (without RBCs), indicating the spectral assignments of individual F-atoms; **B**, 2D EXSY (t_m = 0.5 s) of FDG-234 in the same buffer as **A** and in the presence of RBCs (*Ht* ~50%). All six resonances, visible in **A,** are split into two components: a broader peak, to higher chemical shift, which corresponds to the intracellular resonance (denoted by i); and a sharper peak, corresponding to the extracellular resonance (denoted by e). The cross-peaks, visible in the 2D EXSY spectrum (denoted by *), indicate the exchange between the intra- and extracellular pools. Adapted, with permission of Elsevier, from Ref [77].

Fluoroethylamine is water-soluble and it gives rise to split peaks in ^{19}F NMR spectra of RBC suspensions. By using two-site 1D EXSY analysis, the transmembrane exchange of fluoroethylamine was shown to occur on the sub-second time scale. Inhibition studies allowed us to establish that this compound is transported via the rhesus-associated glycoprotein, as is ammonia [78]. The fluoroethylamine ^{19}F-NMR split peak effect was also used as a means of monitoring cell volume changes in "septicaemia in a test-tube" experiments [79]. The spectra indicated swelling of RBCs followed by lysis, manifested as an initial decrease in peak-separation, followed by collapse of the two peaks into a singlet as the bacteria lysed the RBCs with their enzymic armoury [79].

The general anaesthetic gas halothane gives split peaks in ^{19}F NMR spectra of the brains of halothane-anesthetized rats, although the authors of the studies that showed this did not focus on this feature [80-82]. This peak splitting raises the question as to whether this compound undergoes differential hydrogen bonding inside and outside brain cells, and if spectral changes might be seen in various clinical states. This and many other aspects of the split peak effect remain to be investigated in more detail in the future studies.

7. Conclusions

It has been over 30 years since the separation of intra- and extracellular ^{31}P NMR resonances for a range of (non-titratable) phosphoryl compounds added to RBC suspensions was first observed [2]. This split peak effect can be accounted for by the hypothesis that the high concentration of protein within the RBCs disrupts the extent of hydrogen bonding between the probe compounds and water. Following on from its initial observation in ^{31}P NMR spectra, the effect has subsequently been observed in ^{1}H, ^{13}C, ^{19}F, and ^{133}Cs NMR spectra.

Manifestation of this effect requires a combination of factors: naturally sharp peaks for both intra- and extracellular resonances; sufficiently slow physical exchange between the intra- and extracellular populations of the solute of interest (*i.e.*, slow on the NMR chemical shift time scale); solute-water hydrogen-bond formation; sensitivity of the NMR chemical shift to the extent of hydrogen bonding; and its disruption in the presence of proteins inside relative to outside the cells.

Other nuclides that might have been predicted to display the split peak effect have been studied. Halogens (in analogy to fluorine) might have been expected to show the effect, but at least in $^{35}Cl/^{37}Cl$ NMR, it is not seen since chlorine NMR signals are naturally very broad. In this respect, most quadrupolar nuclei are problematic. However, amongst the alkali metal cations, Cs^+ performs well, showing distinct intra- and extracellular resonances [71]. In this case, it is the *hydrated ion* that putatively interacts with bulk water, and its structure is different in the intra- and extracellular compartments. This suggests an area of study that is beginning to be exploited in measurements of the transport of cations by mechanosensitive ion channels [83].

Past and future applications of the hydrogen-bond-mediated split peak effect abound: these include the measurement of membrane-transport processes (including transmembrane exchange reactions that occur on the sub-second time scale) and monitoring changes in cell volume and/or membrane potential in cells more complicated than RBCs (*e.g.*, [84-86]). With the increasing take-up of RD-DNP [63, 64, 87], hyperpolarized probe molecules that have differential extents of hydrogen bonding in various cell compartments might be used as low-concentration (but high sensitivity) probes of a cell's ionic and metabolic responses to physical and chemical interventions. The study of phenomena such as these in normal and diseased cells (and tissues) will help identify the metabolic features that underlie or are correlated with pathological processes.

Acknowledgements

The work has been supported over many years by the Australian National Health and Medical Research Council (NHMRC), and the Australian Research Council (ARC). Numerous colleagues and graduate students, whose names appears as authors in the references to our own work, are thanked for their contributions to the practice and theoretical aspects of transport kinetics used in exploiting the split peak effect. PWK expresses

appreciation to the University of Sydney for continuing research support as an Emeritus Professor.

References

[1] K. Kirk, Physical Properties of the Human Erythrocyte: Intracellular pH, Transmembrane Potential and Cell Volume, in: Bsc(Hons) Thesis, University of Sydney, NSW, Australia, 1984.
[2] K. Kirk, P.W. Kuchel, Red cell volume changes monitored using a new ^{31}P NMR procedure, J. Magn. Reson., 62 (1985) 568-572.
[3] R.B. Moon, J.H. Richards, Determination of intracellular pH by ^{31}P magnetic resonance, J. Biol. Chem., 248 (1973) 7276-7278.
[4] D.I. Hoult, S.J.W. Busby, D.G. Gadian, G.K. Radda, R.E. Richards, P.J. Seeley, Observation of tissue metabolites using ^{31}P nuclear magnetic resonance, Nature, 252 (1974) 285-287.
[5] P.J. Sims, A.S. Waggoner, C.H. Wang, J.F. Hoffman, Studies on mechanism by which cyanine dyes measure membrane potential in red blood cells and phosphatidylcholine vesicles, Biochemistry, 13 (1974) 3315-3330.
[6] D. Axelrod, Carbocynanine dye orientation in red cell membrane studied by microscopic fluorescence polarization, Biophys. J., 26 (1979) 557-574.
[7] M.H. Levitt, Spin Dynamics, 2nd ed., Wiley-Blackwell, Chichester (England), 2008.
[8] J. Keeler, Understanding NMR Spectroscopy, John Wiley & Sons, Chichester, UK, 2005.
[9] D.G. Gadian, G.K. Radda, R.E. Richards, P.J. Seeley, ^{31}P NMR in living tissue: the road from a promising to an important tool in biology, in: R.G. Shulman (Ed.) Biological Applications of Magnetic Resonance, Academic Press, New York, NY, 1979, pp. 463-535.
[10] K. Kirk, P.W. Kuchel, Equilibrium exchange of dimethyl methylphosphonate across the human red-cell membrane measured using NMR spin transfer, J. Magn. Reson., 68 (1986) 311-318.
[11] K. Kirk, J.E. Raftos, P.W. Kuchel, Triethyl phosphate as an internal ^{31}P NMR reference in biological samples, J. Magn. Reson., 70 (1986) 484-487.
[12] K. Kirk, P.W. Kuchel, R.J. Labotka, Hypophosphite ion as a ^{31}P nuclear magnetic resonance probe of membrane potential in erythrocyte suspensions, Biophys. J., 54 (1988) 241-247.
[13] P.W. Kuchel, W.A. Bubb, S. Ramadan, B.E. Chapman, D.J. Philp, M. Coen, J.E. Gready, P.J. Harvey, A.J. McLean, J. Hook, ^{31}P MAS NMR of human erythrocytes: Independence of cell volume from angular velocity, Magn. Reson. Med., 52 (2004) 663-668.
[14] J.E. Raftos, K. Kirk, P.W. Kuchel, Further investigation of the use of dimethyl methylphosphonate as a ^{31}P NMR probe of red cell volume, Biochim. Biophys. Acta, 968 (1988) 160-166.
[15] K. Kirk, P.W. Kuchel, Red cell volume changes monitored using ^{31}P NMR - a method and model, Studia Biophys., 116 (1986) 139-140.
[16] K. Kirk, Transmembrane Chemical Shift Differences in the ^{31}P NMR Spectra of Erythrocyte Suspensions: Origins and Applications, in: PhD Thesis, University of Sydney, NSW, Australia, 1988.
[17] K. Kirk, P.W. Kuchel, Characterization of transmembrane chemical shift differences in the ^{31}P NMR spectra of various phosphoryl compounds added to erythrocyte suspensions, Biochemistry, 27 (1988) 8795-8802.

[18] M. Cerdonio, A. Congiu-Castellano, L. Calabrese, S. Morante, B. Pispisa, S. Vitale, Room-temperature magnetic properties of oxy- and carbonmonoxyhemoglobin, Proc. Natl Acad. Sci. USA, 75 (1978) 4916-4919.
[19] M. Cerdonio, S. Morante, D. Torresani, S. Vitale, A. DeYoung, R.W. Noble, Reexamination of the evidence for paramagnetism in oxy- and carbonmonoxyhemoglobins, Proc. Natl Acad. Sci. USA, 82 (1985) 102-103.
[20] R.D. Stewart, Effect of carbon monoxide on humans, Ann. Rev. Pharmacol. Toxicol., 15 (1975) 409-423.
[21] S. Wolfram, The *Mathematica* Book, 5th Edition, Wolfram Media Inc., Champaign, IL, 2003.
[22] S.C.K. Chu, Y. Xu, J.A. Balschi, C.S. Springer, Bulk magnetic susceptibility shifts in NMR studies of compartmentalized samples - use of paramagnetic reagents, Magn. Reson. Med., 13 (1990) 239-262.
[23] P.W. Kuchel, B.E. Chapman, W.A. Bubb, P.E. Hansen, C.J. Durrant, M.P. Hertzberg, Magnetic susceptibility: Solutions, emulsions, and cells, Concepts Magn. Reson. A, 18A (2003) 56-71.
[24] C.J. Durrant, M.P. Hertzberg, P.W. Kuchel, Magnetic susceptibility: Further insights into macroscopic and microscopic fields and the sphere of Lorentz, Concepts Magn. Reson. A, 18A (2003) 72-95.
[25] G.E. Maciel, Carbon-13 chemical shifts of carbonyl group. II. A correlation with CO Pi-bond polarity, J. Chem. Phys., 42 (1965) 2746-2751.
[26] G.E. Maciel, J.J. Natterstad, Study of ^{13}C chemical shifts in substituted benzenes, J. Chem. Phys., 42 (1965) 2427-2435.
[27] G.E. Maciel, J.J. Natterstad, Carbon-13 chemical shifts of carbonyl group. III. Solvent effects, J. Chem. Phys., 42 (1965) 2752-2759.
[28] K. Kirk, P.W. Kuchel, Physical basis of the effect of hemoglobin on the ^{31}P NMR chemical shifts of various phosphoryl compounds, Biochemistry, 27 (1988) 8803-8810.
[29] J.D. Dunitz, Organic fluorine: odd man out, ChemBioChem, 5 (2004) 614-621.
[30] C. Dalvit, A. Vulpetti, Weak intermolecular hydrogen bonds with fluorine: Detection and implications for enzymatic/chemical reactions, chemical properties, and ligand/protein fluorine NMR screening, Chem. Europ. J., 22 (2016) 7592-7601.
[31] R.E. London, S.A. Gabel, Determination of membrane potential and cell volume by ^{19}F NMR using trifluoroacetate and trifluoroacetamide probes, Biochemistry, 28 (1989) 2378-2382.
[32] J.R. Potts, A.M. Hounslow, P.W. Kuchel, Exchange of fluorinated glucose across the red-cell membrane measured by ^{19}F-n.m.r. magnetization transfer, Biochem. J., 266 (1990) 925-928.
[33] J.R. Potts, P.W. Kuchel, Anomeric preference of fluoroglucose exchange across human red-cell membranes. ^{19}F-n.m.r. studies, Biochem. J., 281 (1992) 753-759.
[34] A.S.L. Xu, J.R. Potts, P.W. Kuchel, The phenomenon of separate intracellular and extracellular resonances of difluorophosphate in ^{31}P and ^{19}F NMR spectra of erythrocytes, Magn. Reson. Med., 18 (1991) 193-198.
[35] G. Benga, B.E. Chapman, C.H. Gallagher, D. Cooper, P.W. Kuchel, NMR studies of diffusional water permeability of red blood cells from macropodid marsupials (kangaroos and wallabies), Comp. Biochem. Physiol. A-Physiol., 104 (1993) 799-803.

[36] D.J. Philp, W.A. Bubb, P.W. Kuchel, Chemical shift and magnetic susceptibility contributions to the separation of intracellular and supernatant resonances in variable angle spinning NMR spectra of erythrocyte suspensions, Magn. Reson. Med., 51 (2004) 441-444.
[37] A.N. Garroway, Magic angle sample spinning of liquids, J. Magn. Reson., 49 (1982) 168-171.
[38] L.J. Lowe, Free induction decays of rotating solids, Phys. Rev. Lett., 2 (1959) 285-287.
[39] S. Aime, E. Bruno, C. Cabella, S. Colombatto, G. Digilio, V. Mainero, HR-MAS of cells: A "cellular water shift" due to water-protein interactions?, Magn. Reson. Med., 54 (2005) 1547-1552.
[40] C.S. Springer, Physicochemical principles influencing magnetopharmaceuticals, in: R.J. Gillies (Ed.) NMR in Physiology and Biomedicine, Academic Press, San Diego, CA, 1994, pp. 75-100.
[41] K. Kirk, P.W. Kuchel, The contribution of magnetic susceptibility effects to transmembrane chemical shift differences in the ^{31}P NMR spectra of oxygenated erythrocyte suspensions, J. Biol. Chem., 263 (1988) 130-134.
[42] J.H. Chen, B.M. Enloe, Y. Xiao, D.G. Cory, S. Singer, Isotropic susceptibility shift under MAS: The origin of the split water resonances in ^{1}H MAS NMR spectra of cell suspensions, Magn. Reson. Med., 50 (2003) 515-521.
[43] E. Humpfer, M. Spraul, A.W. Nicholls, J.K. Nicholson, J.C. Lindon, Direct observation of resolved intracellular and extracellular water signals in intact human red blood cells using ^{1}H MAS NMR spectroscopy, Magn. Reson. Med., 38 (1997) 334-336.
[44] K. Kirk, NMR methods for measuring membrane transport rates, NMR Biomed., 3 (1990) 1-16.
[45] P.W. Kuchel, Spin-exchange NMR spectroscopy in studies of the kinetics of enzymes and membrane transport, NMR Biomed., 3 (1990) 102-119.
[46] P.W. Kuchel, K. Kirk, G.F. King, NMR methods for measuring membrane transport, in: H.J. Hilderson, G.B. Ralston (Eds.) Subcellular Biochemistry; Physicochemical Methods in the Study of Biomembranes, 1994, pp. 247-327.
[47] M.D. Herbst, J.H. Goldstein, A review of water diffusion measurement by NMR in human red blood cells, Am. J. Physiol., 256 (1989) C1097-C1104.
[48] M.E. Fabry, M. Eisenstadt, Water exchange between red cells and plasma measurement by nuclear magnetic relaxation, Biophys. J., 15 (1975) 1101-1110.
[49] B.E. Chapman, K. Kirk, P.W. Kuchel, Bicarbonate exchange kinetics at equilibrium across the erythrocyte membrane by ^{13}C NMR, Biochem. Biophys. Res. Commun., 136 (1986) 266-272.
[50] K.M. Brindle, F.F. Brown, I.D. Campbell, C. Grathwohl, P.W. Kuchel, Application of spin-echo nuclear magnetic-resonance to whole cell systems - membrane-transport, Biochem. J., 180 (1979) 37-44.
[51] T.R. Eykyn, P.W. Kuchel, Scalar couplings as pH probes in compartmentalized biological systems: ^{31}P NMR of phosphite, Magn. Reson. Med., 50 (2003) 693-696.
[52] R.J. Labotka, A. Omachi, The pH-dependence of red-cell membrane-transport of titratable anions studied by nmr-spectroscopy, J. Biol. Chem., 263 (1988) 1166-1173.
[53] R.J. Labotka, A. Omachi, Erythrocyte anion transport of phosphate analogs, J. Biol. Chem., 262 (1987) 305-311.
[54] J. Andrasko, Measurement of membrane permeability to slowly penetrating molecules by a pulse gradient NMR method, J. Magn. Reson., 21 (1976) 479-484.

[55] J. Andrasko, Water diffusion permeability of human erythrocytes studies by a pulsed gradient NMR technique, Biochim. Biophys. Acta, 428 (1976) 304-311.
[56] A.R. Waldeck, P.W. Kuchel, A.J. Lennon, B.E. Chapman, NMR diffusion measurements to characterise membrane transport and solute binding, Prog. Nucl. Magn. Reson. Spectr., 30 (1997) 39-68.
[57] P.W. Kuchel, B.E. Chapman, J.R. Potts, Glucose transport in human erythrocytes measured using ^{13}C NMR spin transfer, FEBS Lett., 219 (1987) 5-10.
[58] P.W. Kuchel, B.T. Bulliman, B.E. Chapman, K. Kirk, The use of transmembrane differences in saturation transfer for measuring fast membrane-transport - application to HCO_3^- ^{13}C exchange across the human erythrocyte, J. Magn. Reson., 74 (1987) 1-11.
[59] W.S. Price, P.W. Kuchel, Restricted diffusion of bicarbonate and hypophosphite ions modulated by transport in suspensions of red blood cells, J. Magn. Reson., 90 (1990) 100-110.
[60] D. Shishmarev, P.W. Kuchel, NMR magnetization-transfer analysis of rapid membrane transport in human erythrocytes, Biophys. Rev., 8 (2016) 369-384.
[61] U. Himmelreich, K.N. Drew, A.S. Serianni, P.W. Kuchel, C-13 NMR studies of vitamin C transport and its redox cycling in human erythrocytes, Biochemistry, 37 (1998) 7578-7588.
[62] J.R. Potts, B.T. Bulliman, P.W. Kuchel, Urea exchange across the human erythrocyte membrane measured using ^{13}C NMR lineshape analysis, Eur. Biophys. J., 21 (1992) 207-216.
[63] G. Pagès, M. Puckeridge, L. Guo, Y.L. Tan, C. Jacob, M. Garland, P.W. Kuchel, Transmembrane exchange of hyperpolarized ^{13}C-urea in human erythrocytes: sub minute timescale kinetic analysis, Biophys. J., 105 (2013) 1956-1966.
[64] J.H. Ardenkjær-Larsen, B. Fridlund, A. Gram, G. Hansson, L. Hansson, M.H. Lerche, R. Servin, M. Thaning, K. Golman, Increase in signal-to-noise ratio of > 10,000 times in liquid-state NMR, Proc. Natl Acad. Sci. USA, 100 (2003) 10158-10163.
[65] P.W. Kuchel, B.E. Chapman, A.S.L. Xu, Rates of anion transfer across erythrocyte membranes measured with NMR spectroscopy, Prog. Cell Res. (The Band 3 Proteins: Anion Transporters, Binding Proteins and Senescent Antigens. Bamberg, E. and Passow, H. Eds) Elsevier, Amsterdam., 2 (1992) 105-119.
[66] J. Kärger, Determination of diffusion in a 2 phase system by pulsed field gradients, Ann. Phys., 24 (1969) 1-4.
[67] J. Kärger, Influence of 2-phase diffusion on spin-echo attenuation regarding relaxation in measurements using pulsed field gradients, Ann. Phys., 482 (1971) 107-109.
[68] U. Himmelreich, B.E. Chapman, P.W. Kuchel, Membrane permeability of formate in human erythrocytes: NMR measurements, Eur. Biophys. J., 28 (1999) 158-165.
[69] B.P. Shehan, R.M. Wellard, W.R. Adam, D.J. Craik, The use of dietary loading of ^{133}Cs as a potassium substitute in NMR studies of tissues, Magn. Reson. Med., 30 (1993) 573-582.
[70] R.M. Wellard, W.R. Adam, Functional hepatocyte cation compartmentation demonstrated with ^{133}Cs NMR, Magn. Reson. Med., 48 (2002) 810-818.
[71] P.W. Kuchel, D. Shishmarev, M. Puckeridge, M.H. Levitt, C. Naumann, B.E. Chapman, NMR of $^{133}Cs^+$ in stretched hydrogels: One-dimensional, z- and NOESY spectra, and probing the ion's environment in erythrocytes, J. Magn. Reson., 261 (2015) 110-120.
[72] D. Shishmarev, K.I. Momot, P.W. Kuchel, Anisotropic diffusion in stretched hydrogels containing erythrocytes: evidence of cell-shape distortion recorded by PGSE NMR spectroscopy, Magn. Reson. Chem., (2016).
[73] T.M. O'Connell, S.A. Gabel, R.E. London, Anomeric dependence of fluorodeoxyglucose transport in human erythrocytes, Biochemistry, 33 (1994) 10985-10992.

[74] R.E. London, S.A. Gabel, Fluorine-19 NMR studies of glucosyl fluoride transport in human erythrocytes, Biophys. J., 69 (1995) 1814-1818.
[75] E. Dickinson, J.R.P. Arnold, J. Fisher, Determination of glucose exchange rates and permeability of erythrocyte membrane in preeclampsia and subsequent oxidative stress-related protein damage using dynamic-^{19}F-NMR, J. Biomol. NMR, 67 (2017) 145-156.
[76] H.W. Kim, P. Rossi, R.K. Shoemaker, S.G. DiMagno, Structure and transport properties of a novel, heavily fluorinated carbohydrate analogue, J. Am. Chem. Soc., 120 (1998) 9082-9083.
[77] S. Bresciani, T. Lebl, A.M.Z. Slawin, D. O'Hagan, Fluorosugars: synthesis of the 2,3,4-trideoxy-2,3,4-trifluoro hexose analogues of D-glucose and D-altrose and assessment of their erythrocyte transmembrane transport, Chem. Commun., 46 (2010) 5434-5436.
[78] D. Szekely, B.E. Chapman, W.A. Bubb, P.W. Kuchel, Rapid exchange of fluoroethylamine via the rhesus complex in human erythrocytes: ^{19}F NMR magnetization transfer analysis showing competition by ammonia and ammonia analogues, Biochemistry, 45 (2006) 9354-9361.
[79] R. Plummer, J. Bodkin, T.W. Yau, D. Power, N. Pantarat, T.J. Larkin, D. Szekely, W.A. Bubb, T.C. Sorrell, P.W. Kuchel, Modelling *Staphylococcus aureus*-induced septicemia using NMR, Magn. Reson. Med., 58 (2007) 656-665.
[80] A.S. Evers, B.A. Berkowitz, D.A. Davignon, Correlation between the anesthetic effect of halothane and saturable binding in brain, Nature, 328 (1987) 157-160.
[81] A.S. Evers, Correction, Nature, 341 (1989) 766-766.
[82] D.K. Menon, G.G. Lockwood, C.J. Peden, I.J. Cox, J. Sargentoni, J.D. Bell, G.A. Coutts, J.G. Whitwam, In vivo ^{19}F magnetic resonance spectroscopy of cerebral halothane in postoperative patients - preliminary results, Magn. Reson. Med., 30 (1993) 680-684.
[83] P.W. Kuchel, D. Shishmarev, Accelerating metabolism and transmembrane cation flux by distorting red blood cells, Sci. Adv., 3 (2017) eaao1016, 1-10.
[84] Y.H.H. Lien, H.Z. Zhou, C. Job, J.A. Barry, R.J. Gillies, Invivo ^{31}P NMR study of early cellular-responses to hyperosmotic shock in cultured glioma cells, Biochimie, 74 (1992) 931-939.
[85] J.A. Barry, K.A. McGovern, Y.H.H. Lien, B. Ashmore, R.J. Gillies, Dimethyl methylphosphonate (DMMP) - a ^{31}P nuclear magnetic resonance spectroscopic probe of intracellular volume in mammalian cell cultures, Biochemistry, 32 (1993) 4665-4670.
[86] Z.M. Bhujwalla, C.L. McCoy, J.D. Glickson, R.J. Gillies, M. Stubbs, Estimations of intra- and extracellular volume and pH by P-31 magnetic resonance spectroscopy: effect of therapy on RIF-1 tumours, Br. J. Cancer, 78 (1998) 606-611.
[87] G. Pagès, Y.L. Tan, P.W. Kuchel, Hyperpolarized [1,^{13}C]pyruvate in lysed human erythrocytes: effects of co-substrate supply on reaction time courses, NMR Biomed., 27 (2014) 1203-1210.

Glossary

2,3BPG: 2,3-bisphosphoglycerate

DEMP: diethyl methylphosphonate

DFP: difluorophosphate

DMMP: dimethyl methylphosphonate

DNDS: 4 ,4'-dinitrostilbene-2,2'-disulfonic acid

DPP: diphenylphosphinate

FDG-1: 1-fluoro-1-deoxy-D-glucose

FDG-2: 2-fluoro-2-deoxy-D-glucose

FDG-223344: 2,3,4-hexafluoro-2,3,4-trideoxy-D-glucose

FDG-234: 2,3,4-trifluoro-2,3,4-trideoxy-D-glucose

FDG-3: 3-fluoro-3-deoxy-D-glucose

FDG-4: 4-fluoro-4-deoxy-D-glucose

FDG-6: 6-fluoro-6-deoxy-D-glucose

HP: hypophosphite;

Ht: haematocrit

MAS: magic angle spinning

MCV: mean cell volume

NMR: nuclear magnetic resonance

PP: phenylphosphinate

ppm: parts per million

RBC: red blood cell

RD-DNP: rapid dissolution dynamic nuclear polarization

TEP: triethyl phosphate

TMP: trimethyl phosphate

TMPO: trimethylphosphine oxide

VAS: variable angle spinning

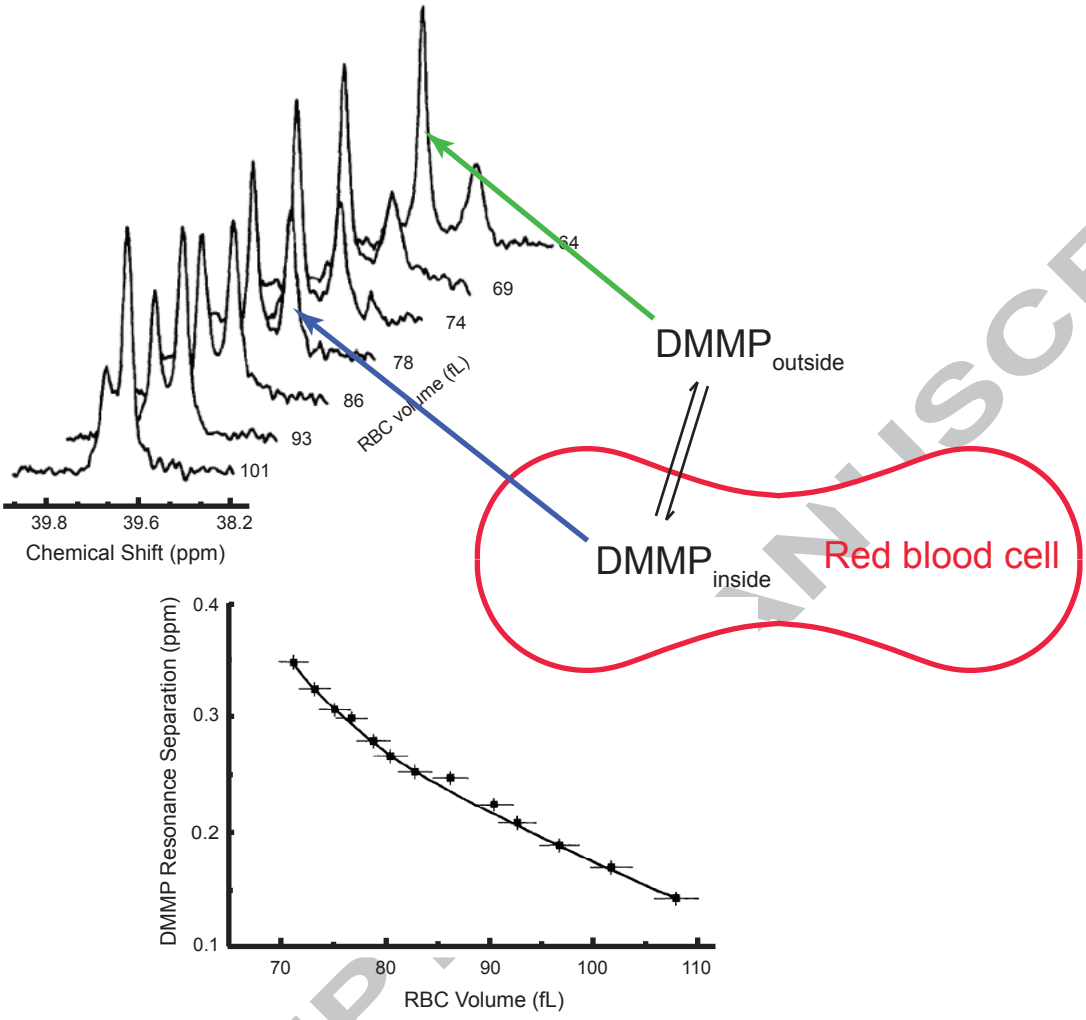

Highlights:

Dimethyl methylphosphonate shows two peaks in ^{31}P NMR spectra of red blood cells

Other phosphonates show the same split peak effect

Mechanism is different average extent of hydrogen bonding inside and outside cells

Enabled first magnetization transfer studies of solute exchange-kinetics in cells

Peak splitting with charged solutes used to measure membrane potential

^{13}C, ^{19}F, $^{133}Cs^{+}$, also have split peaks enabling multiple studies of cell properties